Compact Analytical Description of Digital Radio-Frequency Pulse-Width Modulated Signals

Tanovic, Omer; Ma, Rui

Abstract

Radio frequency pulse-width modulation (RFPWM) has been used as a power coding method in all-digital transmitters, which employ highly efficient switched-mode power amplifiers (SMPA). The main drawback of RF-PWM is the high level of in-band harmonic distortion when digitally implemented. In order to reduce spectral aliasing effects and produce acceptable levels of harmonic noise, ultra-fast clock speeds are required, making it commercially infeasible. In this paper, we derive a novel compact analytical model of a multilevel digital RF-PWM, driven by an arbitrary bounded baseband signal. We show that the spectral aliasing effects are equivalent to a particular amplitude quantization of the input baseband signal. This result implies that highly linear digital RF-PWM can be realized with modest clock speeds if and only if the input baseband signal is prequantized according to the inherent quantization process. We provide full description of this quantization process and describe its dependence on RF-PWM design parameters. Presented results enable a complete understanding of the nonlinear behavior of digitally implemented RF-PWM, and therefore can aid in optimal transceiver design. Numerical simulations in MATLAB were used to verify the derived analytical expressions.

IEEE International Symposium on Circuits & Systems (ISCAS) 2018

Compact Analytical Description of Digital Radio-Frequency Pulse-Width Modulated Signals

Omer Tanovic* †, Rui Ma* and Huifang Sun*

* Mitsubishi Electric Research Laboratories, Cambridge, MA, USA,
† Laboratory for Information and Decision Systems, Department of Electrical Engineering and Computer Science,
Massachusetts Institute of Technology, Cambridge, MA, USA,
Email: otanovic@mit.edu   {rma, hsun}@merl.com

Abstract—**Radio frequency pulse-width modulation (RF-PWM) has been used as a power coding method in all-digital transmitters, which employ highly efficient switched-mode power amplifiers (SMPA). The main drawback of RF-PWM is the high level of in-band harmonic distortion when digitally implemented. In order to reduce spectral aliasing effects and produce acceptable levels of harmonic noise, ultra-fast clock speeds are required, making it commercially infeasible. In this paper, we derive a novel compact analytical model of a multilevel digital RF-PWM, driven by an arbitrary bounded baseband signal. We show that the spectral aliasing effects are equivalent to a particular amplitude quantization of the input baseband signal. This result implies that highly linear digital RF-PWM can be realized with modest clock speeds if and only if the input baseband signal is pre-quantized according to the inherent quantization process. We provide full description of this quantization process and describe its dependence on RF-PWM design parameters. Presented results enable a complete understanding of the nonlinear behavior of digitally implemented RF-PWM, and therefore can aid in optimal transceiver design. Numerical simulations in MATLAB were used to verify the derived analytical expressions.**

I. INTRODUCTION

Switched-mode power amplifiers (SMPA) have gained an increased interest by microwave and communications communities in recent decades, due to their high power efficiency compared to conventional linear PAs [1]-[2]. In addition, SMPAs enable amplification of RF signals while introducing very low distortion into signaling chain. In order to utilize their high efficiency functionality, SMPAs are usually driven by squared (i.e. piece-wise constant) signals taking only a finite number of levels, and therefore require amplitude resolution reduction of standard high resolution RF signals which are to be transmitted. This is commonly achieved by employing radio-frequency pulse width modulation (RF-PWM) [4]-[5], bandpass delta-sigma modulation ($\Delta\Sigma$M) [6], or a combination thereof [7]-[8]. RF-PWM has been shown to be especially interesting due to its achievable high coding efficiency [9]-[10], as compared to $\Delta\Sigma$M which suffers from quantization noise that significantly decreases coding efficiency and requires sharp analog band-pass filters in order to cancel spurious spectral products in the output signal. RF-PWM has been traditionally implemented as a continuous-time or analog system, hence the name analog RF-PWM. In this case, with an appropriate simple pre-distortion, it is possible to achieve high linearity in the signal band of interest. But with transceivers realized for software defined radio (SDR) [11], it is more advantageous for RF-PWM to be fully digitally implemented, in which case it is commonly called digital RF-PWM. Such

scheme can be thought of as a time-sampled version of analog RF-PWM. For that reason, RF-PWM output suffers from high level of in-band harmonic distortion introduced by spectral aliasing effects [12], and very fast sampling clock ($50x f_{RF}$) is needed in order for transceivers to meet the specified linearity requirements. It is clear that having a suitable analytical model of digital RF-PWM could help in better understanding and appropriately mitigating the negative effects introduced by the, above mentioned, leading in-band distortion source.

In this paper, we derive a novel compact and non-trivial closed-form time-domain expression for the output signal of a multilevel digital RF-PWM. Similar to conclusions from [13], this result implies that spectral aliasing effects can be described in time-domain as a suitable amplitude quantization of the baseband input signal. We provide a full description of this quantization process and describe its dependence on RF-PWM design parameters. The result suggests that highly linear digital RF-PWM can be realized with modest clock speeds if and only if the input baseband signal is pre-quantized according to the inherent quantization process. Due to space limitations, derivations for a 3-level RF-PWM are only presented. To author's best knowledge this is the first reported analytical description of a digital RF-PWM system. The result greatly simplifies spectral analysis of RF-PWM signals, and provides a framework for the design of very linear digital transceivers that work at reasonable clock speeds and still utilize the full advantage of highly power efficient RF-PWM.

II. THE PRINCIPLE OF OPERATION OF RF-PWM

In this section the method of operation of what is defined as analog or continuous-time RF-PWM is described, and an analytical model, though without derivation, is given (detailed derivation can be found in e.g. [3]).

The main idea of RF-PWM is to modulate an RF signal into a stream of unipolar or bipolar pulses, where the envelope and phase are represented by the width and timing of the pulses. In 3-level RF-PWM schemes, a baseband input signal is first upconverted to RF frequency, and the modulated carrier is then compared to a fixed threshold value to produce a pulsed output train [1], as shown in Fig. 1. Let $a(t)$ be the baseband input signal and $x(t) = a(t)\cos(2\pi f_c t)$ the modulated RF carrier, where f_c is the RF or carrier frequency, and $\omega_c = 2\pi f_c$. Also, let $y(t)$ be the pulsed output train, and v_{th} the value of the RF-PWM threshold. This threshold value v_{th} is a parameter of the RF-PWM system, and is chosen in accordance with the expected input signal amplitude range in such a way that

$|v_{th}| < \max_t |a(t)|$ is satisfied. Now, RF-PWM output signal $y = y(t)$ is generated according to the following formula

$$y(t) = \begin{cases} 1, & x(t) > v_{th} \\ 0, & |x(t)| \leq v_{th} \\ -1, & x(t) < v_{th} \end{cases} . \quad (1)$$

In the above expression, non-zero values of the output signal are normalized to ± 1, but in general, can be set to any desired value (they do not even have to be equal). This process of generating output signal $y(t)$ is shown in Fig. 2, for an arbitrary choice of input signal $a(t)$. As can be seen from Fig. 2, signal $y(t)$ is a sequence of alternating pulses, where the width of each pulse depends on the value of envelope $a(t)$ of the RF carrier signal $x(t)$. Let us denote this width signal as $d(t)$ (to be more precise, for mathematical convenience, we denote with $d(t)$ a half of the actual width). 2). It has been shown (see e.g. [3]) that the following relationship between $a(t)$ and $d(t)$ holds

$$d(t) = \begin{cases} -\frac{1}{\pi} \arccos \frac{v_{th}}{|a(t)|}, & a(t) < -v_{th} \\ 0, & |a(t)| \leq v_{th} \\ \frac{1}{\pi} \arccos \frac{v_{th}}{|a(t)|}, & a(t) > v_{th} \end{cases} . \quad (2)$$

With $d(t)$ as defined above, it can be shown (see e.g. [3]) that the output $y(t)$ of the analog RF-PWM system can be expressed as

$$y(t) = \frac{4 \sin(\pi d(t))}{\pi} \cos(\omega_c t) +$$
$$+ \sum_{k=2}^{\infty} \frac{4 \sin(\pi(2k-1)d(t))}{\pi(2k-1)} \cos((2k-1)\omega_c t). \quad (3)$$

It is clear from (3) that output $y(t)$ is a quasi-harmonic signal, with the fundamental component at the carrier frequency f_c. Moreover, since $a(t)$ is modulating a cosine, due to symmetry, only odd harmonics are present. This is very advantageous, since spectral regrowth coming from higher order harmonics is not going to affect much the RF signal band (i.e. frequency band around f_c), and can be easily taken care of by applying a relatively cheap analog band-pass filter. By appropriately pre-distorting baseband signal $a(t)$, it is possible to invert the nonlinear AM-AM characteristic of the RF-PWM (from $a(t)$ to the first harmonic), and achieve (almost) linear mode of operation [4].

In general, an RF-PWM scheme with $2M + 1$ levels is defined in a similar way. Now instead of having just one threshold there are going to be M different threshold values v_{th}^i, for $i = \{1, \ldots, M\}$, where without loss of generality we assume $v_{th}^i < v_{th}^j$ for all $i < j$ (otherwise it is always possible to re-order the thresholds so that this is satisfied). In this case, input RF signal $x(t)$ is compared to each threshold v_{th}^i to generate a pulsed signal $y_i(t)$, and the RF-PWM output is formed by summing (and possibly scaling) all $y_i(t)$.

III. DIGITAL RF-PWM

The operation of digital RF-PWM can be defined in a way similar to what was described in the previous section for analog RF-PWM. Let $\tilde{a} = \tilde{a}[n]$ be an arbitrary real-valued and bounded signal, and let $v_{th} > 0$ such that $v_{th} < \max_n |\tilde{a}[n]|$. Also, let $N > 1$ be an integer, and let us define signal
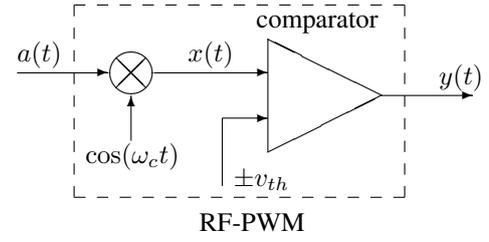
Fig. 1. Principle block diagram of CT RF-PWM describing the output signal generation.
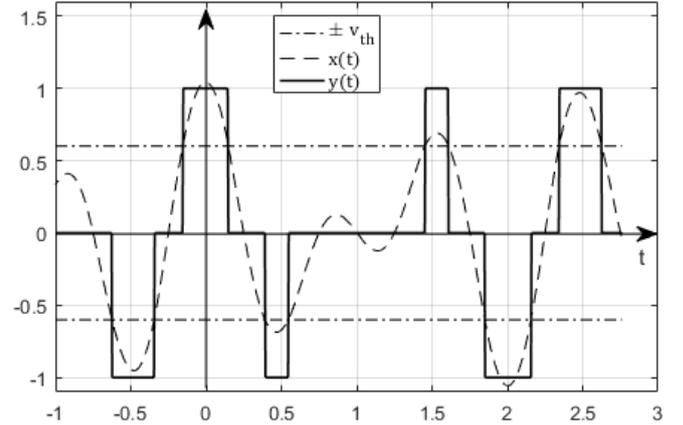
Fig. 2. An example of output signal generation in three-level digital RF PWM.

$\tilde{x} = \tilde{x}[n] = \tilde{a}[n] \cos\left(\frac{2\pi n}{N}\right)$. Analogously to (1), the output $\tilde{y}[n]$ of a 3-level digital RF-PWM system can now be defined as

$$\tilde{y}[n] = \begin{cases} 1, & \tilde{x}[n] > v_{th} \\ 0, & |\tilde{x}[n]| \leq v_{th} \\ -1, & \tilde{x}[n] < v_{th} \end{cases} . \quad (4)$$

It is clear that digital RF-PWM can be seen as a sampled version of analog RF-PWM if the sampling frequency f_s is chosen such that $f_s = N \cdot f_c$. In this case digital frequency $2\pi/N$ corresponds to the carrier frequency f_c. Now we use the above definition of digital RF-PWM to find an expression for $\tilde{y}[n]$ in terms of $\tilde{a}[n]$, similar to (3) for $y(t)$ and $a(t)$. Without loss of generality we assume that the oversampling ratio N is an integer, which is true in most practical applications. Due to space constraints, we present derivation of the analytical model of digital RF-PWM only for odd values of N (derivation for even values of N follows in a similar way). For a given $\tilde{a}[n]$, let us define signal $\tilde{d}[n]$ as

$$\tilde{d}[n] = \begin{cases} -\frac{1}{\pi} \arccos \frac{v_{th}}{|\tilde{a}[n]|}, & \tilde{a}[n] < -v_{th} \\ 0, & |\tilde{a}[n]| \leq v_{th} \\ \frac{1}{\pi} \arccos \frac{v_{th}}{|\tilde{a}[n]|}, & \tilde{a}[n] > v_{th} \end{cases} . \quad (5)$$

The input-output analytical model of a digital RF-PWM system is now given by the following theorem.

Theorem 1: Let $(\tilde{a}, \tilde{y})$ be the input-output pair of a 3-level digital RF-PWM system with threshold $v_{th} > 0$ and digital carrier frequency $2\pi/N$, $N > 1, N \in \mathbb{N}$ and N odd. The

following input-output relation holds

$$\tilde{y}[n] = \tilde{y}_0[n] + \sum_{k=1}^{\frac{N-1}{2}} \tilde{y}_k[n] \cos\left(\frac{2\pi(2k-1)n}{N}\right), \quad (6)$$

where

$$\tilde{y}_0[n] = \begin{cases} \frac{1}{N}, & i - \text{even} \\ -\frac{1}{N}, & i - \text{odd} \end{cases}$$

$$\tilde{y}_k[n] = \frac{2\sin\left(\pi(2k-1)\frac{2i+1}{2N}\right)}{N\sin\left(\frac{\pi(2k-1)}{2N}\right)} \quad (7)$$

when $\tilde{d}[n] \in \left(\frac{i}{N}, \frac{i+1}{N}\right]$ and $\forall i \in \left\{\left\lfloor -\frac{N}{2}\right\rfloor, \ldots, \left\lfloor\frac{N}{2}\right\rfloor\right\}$.

Proof: Let us first state the following Lemma (proof of which can be found in e.g. [13]), which will be used in the proof of Theorem 1.

Lemma 2: Let $d \in \left(-\frac{1}{2}, \frac{1}{2}\right)$, $m \in \left\{1, \ldots, \left\lfloor\frac{M-1}{2}\right\rfloor\right\}$ and $M \in \mathbb{N}$, $M > 1$. Then the following equalitites hold

$$\sum_{n=-\infty}^{\infty} \frac{\sin(\pi M n d)}{\pi M n} = \frac{2i+1}{M}, \quad (8)$$

$$\sum_{n=-\infty}^{\infty} \frac{\sin(\pi(Mn+m)d)}{\pi(Mn+m)} = \frac{\sin\left(\pi m\frac{2i+1}{M}\right)}{M\sin\left(\frac{\pi m}{M}\right)}, \quad (9)$$

when $d \in \left(\frac{2i}{M}, \frac{2i+2}{M}\right]$, $\forall i \in \left\{\left\lfloor -\frac{M}{4}\right\rfloor, \ldots, \left\lfloor\frac{M}{4}\right\rfloor\right\}$.

As previously noted, the output $\tilde{y}[n]$ of digital RF-PWM can be thought of as a result of sampling of the output $y(t)$ of the equivalent analog RF-PWM, where the corresponding sampling frequency is $f_s = N \cdot f_c$. From (2) it follows that $\tilde{y}[n]$ can be expressed as

$$\tilde{y}[n] = y(nT_s) = \sum_{k=1}^{\infty} \frac{4\sin((2k-1)\pi\tilde{d}[n])}{\pi(2k-1)} \cos\left(\frac{2\pi(2k-1)n}{N}\right), \quad (10)$$

where $T_s = 1/f_s$ and $\tilde{d}[n]$ is defined in (5). Due to an integer period of the discrete cosine in (10), it follows that there are only finitely many unique harmonics, and therefore the infinite sum in (10) can be simplified to a finite sum. By careful examination of digital frequencies in (10), it can be noticed that only DC component and odd harmonics exist, and thus the total number of harmonics is equal to $(N+1)/2$. It follows that signal $\tilde{y}[n]$ can be expressed as

$$\tilde{y}[n] = \tilde{y}_0[n] + \sum_{k=1}^{\frac{N-1}{2}} \tilde{y}_k[n] \cos\left(\frac{2\pi(2k-1)n}{N}\right), \quad (11)$$

where

$$\tilde{y}_0[n] = \sum_{l=1}^{\infty} \frac{4\sin(\pi N(2l-1)\tilde{d}[n])}{\pi N(2l-1)},$$

$$\tilde{y}_k[n] = \sum_{l=0}^{\infty} \frac{4\sin(\pi(2Nl+2k-1)\tilde{d}[n])}{\pi(2Nl+2k-1)} + \quad (12)$$

$$+ \sum_{l=1}^{\infty} \frac{4\sin(\pi(2Nl+2N-2k+1)\tilde{d}[n])}{\pi(2Nl+2N-2k+1)}.$$

Here $\tilde{y}_0$ denotes the baseband component of $\tilde{y}$, and $\tilde{y}_k$ are higher order harmonics, similar to the description of analog PWM output, given in (3). It is now clear that aliasing effects manifest in (12) in terms of an infinite number of additional summands. Let us now simplify expressions in (12). DC component $\tilde{y}_0$ can be rewritten as

$$\tilde{y}_0[n] = \sum_{l=-\infty}^{\infty} \frac{2\sin(\pi N(2l-1)\tilde{d}[n])}{\pi N(2l-1)} =$$

$$= 2\sum_{l=-\infty}^{\infty} \frac{\sin(\pi Nl\tilde{d}[n])}{\pi Nl} - 2\sum_{l=-\infty}^{\infty} \frac{\sin(2\pi Nl\tilde{d}[n])}{2\pi Nl}. \quad (13)$$

In a similar way, expression for $\tilde{y}_k$ in (12) can be rewritten as

$$\tilde{y}_k[n] = 4 \cdot \sum_{l=-\infty}^{\infty} \frac{\sin(\pi(2Nl+2k-1)\tilde{d}[n])}{\pi(2Nl+2k-1)}. \quad (14)$$

It can be observed from (13) and (14) that expressions for harmonics of signal $\tilde{y}[n]$ involve only infinite sums of discrete sinc functions, which can be computed analytically, as given in Lemma 2. For the two sums in (13) we have

$$\sum_{l=-\infty}^{\infty} \frac{\sin(\pi Nl\tilde{d}[n])}{\pi Nl} = \frac{2i+1}{N}, \quad (15)$$

when $\tilde{d}[n] \in \left(\frac{2i}{N}, \frac{2i+2}{N}\right]$ and $\forall i \in \mathcal{I} = \left\{\left\lfloor -\frac{N}{4}\right\rfloor, \ldots, \left\lfloor\frac{N}{4}\right\rfloor\right\}$, and

$$\sum_{l=-\infty}^{\infty} \frac{\sin(2\pi Nl\tilde{d}[n])}{2\pi Nl} = \frac{2m+1}{2N}, \quad (16)$$

when $\tilde{d}[n] \in \left(\frac{m}{N}, \frac{m+1}{N}\right]$ and $\forall m \in \mathcal{M} = \left\{\left\lfloor -\frac{N}{2}\right\rfloor, \ldots, \left\lfloor\frac{N}{2}\right\rfloor\right\}$. Therefore, $\tilde{y}_0[n]$ can be expressed as

$$\tilde{y}_0[n] = \frac{4i-2m+1}{N}, \quad (17)$$

where i and m depend on the value of $\tilde{d}[n]$, as given above. It is not hard to see that for each even value of $m \in \mathcal{M}$ there exists an $i \in \mathcal{I}$ such that $i = m/2$. Similarly, for each odd value of $m \in \mathcal{M}$ there exists an $i \in \mathcal{I}$ such that $i = (m-1)/2$. It now follows from (17) that for all $m \in \mathcal{M}$ when $\tilde{d}[n] \in \left(\frac{m}{N}, \frac{m+1}{N}\right]$ we have

$$\tilde{y}_0[n] = \begin{cases} \frac{1}{N}, & m - \text{even} \\ -\frac{1}{N}, & m - \text{odd} \end{cases}. \quad (18)$$

This completes the proof for $\tilde{y}_0[n]$.

A closed-form expression for $\tilde{y}_k[n]$ is obtained by applying results of Lemma 2 (for $M = 2N$ and $m = 2k - 1$) on (14). Therefore, it follows that

$$\tilde{y}_k[n] = \frac{2\sin\left(\pi(2k-1)\frac{2i+1}{2N}\right)}{N\sin\left(\frac{\pi(2k-1)}{2N}\right)} \quad (19)$$

when $\tilde{d}[n] \in \left(\frac{i}{N}, \frac{i+1}{N}\right]$ and $\forall i \in \left\{\left\lfloor -\frac{N}{2}\right\rfloor, \ldots, \left\lfloor\frac{N}{2}\right\rfloor\right\}$.

This concludes the proof. ∎

It can be seen from (5) and (19) that k-th harmonic $\tilde{y}_k$ can be written as

$$\tilde{y}_k[n] = \frac{2\sin\left(\pi(2k-1)\tilde{d}_Q[n]\right)}{N\sin\left(\frac{\pi(2k-1)}{2N}\right)}, \quad (20)$$

where $\tilde{d}_Q[n] = (\mathbf{Q}\tilde{d})[n]$ and $\mathbf{Q}$ is a uniform quantizer with $N + 1$ output levels on the interval $(-0.5, 0.5)$, and an additional level (or fixed point) at 0 (i.e. $\tilde{d}[n] = 0$ implies $\tilde{d}_Q[n] = 0$). Therefore, in total, $\mathbf{Q}$ has $N_Q = N + 2$ output levels. We call this quantization process *the hidden quantization*, in order to distinguish it from the main quantization which is the very operation of RF-PWM.

We now discuss some consequences of this result. Intuitively it is clear that increasing the oversampling rate and/or the number of levels/thresholds in RF-PWM, the linearity performance increases, due to either less aliasing effects (higher oversampling rate) or better amplitude resolution of the output signal (more levels of RF-PWM). A common conclusion in the literature is that in order to use RF-PWM as a power coder in all-digital transmitters (ADT), the sampling frequency has to be orders of magnitude larger than the carrier frequency [10]. This is explained by the high levels of in-band distortion introduced by aliasing if the ratio $N = f_s/f_c$ is too small. Generally, this is true if signal taking arbitrary amplitude values is fed into RF-PWM. The input-output model from Theorem 1 suggests that major portion of the in-band distortion is entirely due to the hidden quantization of the RF-PWM input signal. This implies that if the RF-PWM input signal was already quantized, there would be no additional distortion introduced by the hidden quantization. In other words, the RF-PWM output signal would be truly alias-free. It is important to emphasize that no aliasing will occur if and only if the input signal amplitudes correspond exactly to output levels of the hidden quantizer $\mathbf{Q}$, as defined above. But pre-quantization of the high-resolution true input signal would introduce distortion itself, with or without RF-PWM, thus possibly diminishing the gain of aliasing-free RF-PWM. But now ADT designer has some control over the quantization process that should be applied to the input signal. Hence quantization noise can be shaped to the out-of-band region with e.g. $\Delta\Sigma M$, controlling in-band distortion of the RF-PWM output. In such a way, highly linear ADTs can be designed as recently reported in [14].

IV. Simulation Results

In this section, aided by MATLAB simulations, we validate the derived analytical model of digital RF-PWM. Simulations were performed for two cases of RF-PWM input signals and a wide range of RF-PWM parameters.

In the first case, envelope of a randomly generated 100MHz-bandwidth 64QAM signal is used as the input into digital RF-PWM with carrier frequency $f_c = 1$GHz. In the second case, the in-phase component of a 50MHz-bandwidth LTE signal is used as the input signal, and the carrier frequency was set to 2GHz. The oversampling ratio N and the number of threshold signals M were varied. As a measure of performance, normalized RMSE between the output obtained by comparison of the input signal with thresholds, and the one obtained from the novel analytical model, was used.

Validation error values for various combinations of N and M are shown in Table I. It is clear that the error is negligible, and is not identicaly zero only due to the finite precision of numerical calculations in MATLAB. This confirms the validity of the derived analytical model of digital RF-PWM.

TABLE I. MODEL VALIDATION ERROR FOR VARIOUS VALUES OF THE OVERSAMPLING RATIO N AND THE NUMBER OF THRESHOLDS M (CONSEQUENTLY, $2M + 1$ IS THE NUMBER OF OUTPUT LEVELS). ALL VALUES ARE IN PARTS-PER-TRILLION.

64QAM input signal						
$2M+1$ \ N	3	4	5	6	7	8	9
3	19.1	7.69	8.31	9.56	7.19	4.32	8.79
5	19.8	7.65	7.02	9.92	5.83	4.3	7.19
7	20.2	7.74	6.59	10.1	4.77	4.15	5.51
9	20.2	7.69	6.53	10.09	4.71	4.11	5.23

LTE input signal						
$2M+1$ \ N	3	4	5	6	7	8	9
3	38.22	15.36	16.81	19.11	14.53	8.6	17.76
5	38.75	15.29	13.9	19.37	10.58	8.55	13.07
7	40,11	15.41	13.21	20.06	9.74	8.21	11.08
9	40.63	15.49	13.46	20.31	9.64	8.26	10.52
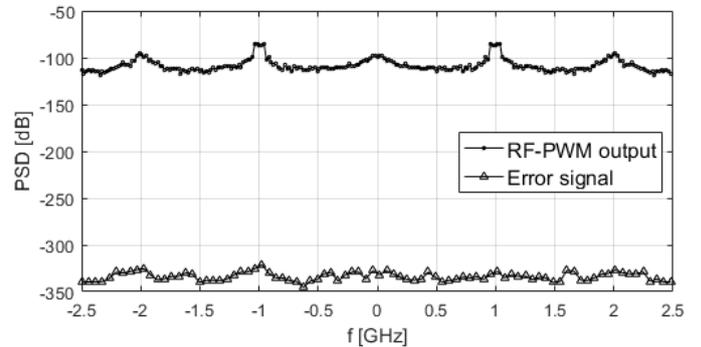
Fig. 3. An example of PSD of digital RF-PWM output and error signals.

As an illustration, spectra of the simulation obtained output signal of digital RF-PWM, driven by the 64QAM input, and the corresponding model validation error signal, are depicted in Fig. 3. It can be seen that power of the error signal is substantially lower than the output signal power, as was expected from the results presented in Table I.

V. Conclusion

In this paper, a compact analytical model of a digital radio-frequency pulse-width modulation system was presented. It was shown that the input signal is subject to an additional quantization process (dubbed 'the hidden quantization'), which is a time-domain manifestation of spectral-aliasing effects that are intrinsic to digital PWM mode of operation. This result implies that highly linear digital RF-PWM can be realized with modest clock speeds if and only if the input signal is appropriately pre-quantized (e.g. with a $\Delta\Sigma M$) according to the inherent 'hidden' quantization process. A full description of the hidden quantization was provided and its dependence on RF-PWM design parameters was described. Presented results enable a complete understanding of the nonlinear behavior of a digitally realized RF-PWM, and can aid in optimal transceiver design. Numerical simulations in MATLAB were used to verify the derived analytical expressions.

REFERENCES

[1] F. H. Raab,"Class-D power amplifier with RF pulse-width modulation," *Dig. IEEE Microw. Theory Tech. Sym.*, pp. 924-927, June 2010.

[2] M. Eron, B. Kim, F. Raab, R. Caverly and J. Staudinger, "The Head of the Class," *in IEEE Microwave Magazine*, vol. 12, no. 7, pp. S16-S33, Dec. 2011.

[3] F. H. Raab, "Radio frequency pulsewidth modulation," *IEEE Trans. Commun.*, vol. COM-21, no. 8, pp. 958-966, Aug. 1973.

[4] M. Nielsen and T. Larsen, "An RF Pulse Width Modulator for Switch-Mode Power Amplification of Varying Envelope Signals," *2007 Topical Meeting on Silicon Monolithic Integrated Circuits in RF Systems*, Long Beach, CA, 2007, pp. 277-280.

[5] C. Haslach, D. Markert, A. Frotzscher and A. Pascht, "New efficient architectures for RF pulse width modulators," *2013 IEEE MTT-S International Microwave Symposium Digest (MTT)*, Seattle, WA, 2013, pp. 1-4.

[6] T. Johnson and S. P. Stapleton,"RF class-D amplification with bandpass sigma-delta modulator drive signals," *IEEE Trans. Circuits Syst. I*, vol. 53, no. 12, pp. 25072520, Dec. 2006.

[7] D. Markert, C. Haslach, H. Heimpel, A. Pascht and G. Fischer, "Phase-modulated DSM-PWM hybrids with pulse length restriction for switch-mode power amplifiers," *2014 44th European Microwave Conference*, Rome, 2014, pp. 1364-1367.

[8] S. Chung, R. Ma, S. Shinjo, H Nakamizo, K. Parsons and K. H. Teo, "Concurrent Multiband Digital Outphasing Transmitter Architecture Using Multidimensional Power Coding," *IEEE Trans. Microw. Theory Techn.*, vol 63, no. 2, pp. 598-613, Feb. 2015.

[9] D. Markert, C. Haslach, G. Fischer and A. Pascht, "Coding efficiency of RF pulse-width-modulation for mobile communications," *2012 International Symposium on Signals, Systems, and Electronics (ISSSE)*, Potsdam, 2012, pp. 1-5.

[10] Q. Zhu, R. Ma, C. Duan, K. H. Teo and K. Parsons, "A 5-level discrete-time power encoder with measured coding efficiency of 70% for 20-MHz LTE digital transmitter," *2014 IEEE MTT-S International Microwave Symposium (IMS2014)*, Tampa, FL, 2014, pp. 1-3.

[11] F. Ghannouchi, "Power Amplifier and Transmitter Architectures for Software Defined Radio Systems," *IEEE Circuits Syst. Mag.*, vol. 10, no. 4, pp. 56-63, Nov. 2010

[12] S. Santi, R. Rovatti, and G. Setti, "Spectral aliasing effects of PWM signals with time-quantized switching instants," *2004 IEEE International Symposium on Circuits and Systems*, 2004, pp. IV-689-92 Vol.4.

[13] O. Tanovic, R. Ma, and K. H. Teo, "Theoretical Bounds on Time-Domain Resolution of Multilevel Carrier-Based Digital PWM Signals Used in All-Digital Transmitters," *IEEE 60th International Midwest Symposium on Circuits and Systems (MWSCAS) 2017*, Boston, MA, 2017, pp. 1146-1149.

[14] O. Tanovic and R. Ma, "Truly Aliasing-Free Digital RF-PWM Power Coding Scheme for Switched-Mode Power Amplifiers," *2018 IEEE Radio and Wireless Symposium (RWS)*, Anaheim, CA, 2018, pp. 68-71.